*Inorg. Chem.* **2007**, *46*, 10539–10548


# Predicting Exchange Coupling Constants in Frustrated Molecular Magnets Using Density Functional Theory

**Indranil Rudra, Qin Wu, and Troy Van Voorhis***

*Department of Chemistry, Massachusetts Institute of Technology, 77 Massachusetts Avenue, Cambridge, Massachusetts 02139*

Received May 6, 2007

We study the Heisenberg exchange couplings in polynuclear transition-metal clusters with strong spin frustration using a variety of theoretical techniques. We present results for a trinuclear $Cr^{III}$ molecule, a tetranuclear $Fe^{III}$ complex, and an octanuclear $Fe^{III}$ molecular magnet. We explore the physics of the exchange couplings in these systems using standard broken-symmetry (BS) techniques and a more recently developed constrained density functional theory (C-DFT) approach. The calculations show that the expected picture of localized spin moments on the metal centers is appropriate, and in each case C-DFT predicts coupling constant values in good agreement with experiment. Furthermore, we demonstrate that all of the C-DFT spin states for a given cluster can be reasonably described by a single Heisenberg Hamiltonian. These findings are significant in part because standard BS calculations are in conflict with the experiments on a number of key points. For example, BS-DFT predicts a doublet (rather than quartet) ground state for the $Cr^{III}$ cluster while for the $Fe^{III}$ complexes BS-DFT predicts some of the exchange couplings to be ferromagnetic whereas the experimentally derived couplings are all antiferromagnetic. Furthermore, for BS-DFT the best-fit exchange parameters can depend significantly on the set of spin configurations chosen. For example, by choosing configurations with $M_S$ closer to $M_S^{max}$ the BS-DFT couplings can typically be made somewhat closer to the C-DFT and experimental results. Thus, in these cases, our results consistently support the experimental findings.

## I. Introduction

The present interest in transition-metal-based molecular magnets is driven by their potential application as next-generation magnetic data storage devices.[1] For these applications, molecular magnets with high ground-state spin and easy axis anisotropy are the ideal targets. However, the synthesis of compounds with these properties is an extremely challenging task. The majority of the high-spin anisotropic clusters synthesized until now are based on 3d transition metals, mainly Mn and Fe.[2−6] Recently, some progress has been reported in synthesizing highly magnetic clusters with other transition metals and lanthanides.[7−10] Numerous attempts have been made to join highly anisotropic fragments to synthesize a cluster with global anisotropy. Until very recently[11] the $Mn_{12}$−acetate cluster with anisotropy barrier of 56 K[12] was still the best molecular magnet synthesized. Further improvement rests on a microscopic understanding of the exchange coupling mechanism and magnetostructural correlations.

* To whom correspondence should be addressed. E-mail: tvan@mit.edu.

(1) Ritter, S. K. *Chem. Eng. News* **2004**, *82* (50), 29−32.
(2) Gunther, L.; Barbara, B. *Quantum Tunneling of Magnetization−QTM '94*; NATO ASI Series; Kluwer: Dordrecht, The Netherlands, 1995; Vol. 301.
(3) Powell, A.; Heath, S.; Gatteschi, D.; Pardi, L.; Sessoli, R.; Spina, G.; del Giallo, F.; Pieralli, F. *J. Am. Chem. Soc.* **1995**, *117*, 2491−2502.
(4) Gatteschi, D.; Sessoli, R. *Angew. Chem., Int. Ed.* **2003**, *42*, 268−297.
(5) He, G. J.; Zhang, X. Y.; Duan, C. Y. *Chin. J. Inorg. Chem.* **2006**, *22*, 691−695.
(6) Grapperhaus, C. A.; O'Toole, M. G.; Mashuta, M. S. *Inorg. Chem. Commun.* **2006**, *9*, 1204−1206.
(7) Sokol, J. J.; Hee, A. G.; Long, J. R. *J. Am. Chem. Soc.* **2002**, *124*, 7656−7657.
(8) Choi, H. J.; Sokol, J. J.; Long, J. R. *Inorg. Chem.* **2004**, *43*, 1606−1608.
(9) van Slageren, J.; Sessoli, R.; Gatteschi, D.; Smith, A. A.; Helliwell, M.; Winpenny, R. E. P.; Cornia, A.; Barra, A. L.; Jansen, A. G. M.; Rentschler, E.; Timco, G. A. *Chem.−Eur. J.* **2002**, *8*, 277−285.
(10) Schelter, E. J.; Prosvirin, A. V.; Dunbar, K. R. *J. Am. Chem. Soc.* **2004**, *126*, 15004−15005.
(11) Milios, C. J.; Vinslava, A.; Wernsdorfer, W.; Moggach, S.; Parsons, S.; Perlepes, S. P.; Christou, G.; Brechin, E. K. *J. Am. Chem. Soc.* **2007**, *125*, 2754−2755.
(12) Friedman, J. R.; Sarachik, M. P.; Tejada, J.; Ziolo, R. *Phys. Rev. Lett.* **1996**, *76*, 3830−3833.

10.1021/ic700871f CCC: $37.00 
Published on Web 11/14/2007

In transition-metal complexes, exchange coupling is adequately described by a Heisenberg Hamiltonian due to the localized nature of the 3d electrons.

$$\hat{H} = -\sum_{ij} J_{ij}\mathbf{S}_i\cdot\mathbf{S}_j \quad (1)$$

The magnitude and sign of the exchange coupling parameter $J_{ij}$ give the coupling strength between metal spins on sites *i* and *j* and the nature of the spin interaction (e.g., ferromagnetic or antiferromagnetic), respectively. Competing exchange pathways lead to geometrically induced spin frustration, which is a common occurrence in polynuclear transition-metal clusters. In the presence of frustration, the accurate prediction of the ground spin state becomes a nontrivial task as it depends on the nature and relative strengths of all the exchange interactions. Further, spin frustration in these clusters often results in closely spaced low-lying energy levels whose ordering is sensitive to the value of exchange couplings. Due to this sensitivity, spin frustration often leads to interesting high-spin magnetic ground states with an anisotropy that is tunable via structural modifications.[13] Thus, by controlling the extent and nature of spin frustration we can, in principle, control the magnetic properties of the clusters. In addition, the ability of many spin-frustrated complexes to switch easily between different magnetic states has opened up the possibility of their application to various magnetic device purposes.[1]

In this paper, we use density functional theory (DFT) techniques to explore the exchange couplings in several polynuclear metal clusters with significant spin frustration. DFT is the method of choice for obtaining exchange couplings of large clusters in an *ab initio* manner. However, frustrated transition-metal clusters pose a significant challenge for DFT because the competing spin interactions usually lead to near-degeneracy effects. As a result, the ground spin state usually involves many configurations, which are extremely difficult to describe in a DFT framework.[14,15] Furthermore, because of the closely spaced energy level structure, the relative energy levels of different spin configurations must be determined very accurately if the results are to be even qualitatively correct. It is therefore not surprising that there are relatively few applications of DFT to frustrated magnetic systems reported in the literature.[16−20] In the context of this paper, we will employ two different approaches to computing the exchange coupling. In DFT, one typically uses a broken-symmetry (BS) description of the low-spin (LS) state, originally proposed by Noodleman.[21] Modifications of this method have been proposed that offer certain advantages over the original formalism,[22,23] but in all cases the BS state is the central object. Recently, we have proposed an alternative approach in which constrained DFT (C-DFT) is used to construct the energy of the uncoupled spin, or Ising, configurations (e.g., $\uparrow\downarrow$, $\uparrow\uparrow$) directly.[24] This method has been shown to give very accurate exchange couplings for several binuclear transition-metal complexes.[24] In this Article, we turn our attention to geometrically induced spin frustration and focus on three different systems: a trinuclear $Cr^{III}$ molecule, a tetranuclear $Fe^{III}$ complex, and an octanuclear $Fe^{III}$ molecular magnet. We find that C-DFT gives a good description of the experimentally derived exchange couplings in each cluster, while BS-DFT differs from experiment in several important respects. By exploring the exchange couplings in these complexes, we show that the low-lying C-DFT states can be described using a single Heisenberg Hamiltonian based on localized magnetic moments in every case. Thus, C-DFT provides a physically reasonable *ab initio* interpretation of the spin state structure of these frustrated magnets.

## II. Theoretical Overview

In the Kohn−Sham (KS) formulation,[25] DFT uses a fictitious single determinant reference to represent the density of the system. This is problematic for open-shell multiplets, which require a multideterminant wavefunction for a qualitatively correct picture.[14,15] Indeed, using existing functionals, one typically encounters spin-contaminated BS determinants in calculations on open-shell multiplets. The basic idea of the original BS-DFT approach is to treat these BS solutions as approximate Ising-like configurations in order to compute the exchange coupling.[21,26] This means that for a molecule A−B, BS-DFT mimics the singlet by a single determinantal BS solution which has excess α spin on A and excess $\beta$ spin on B. In comparison, the high-spin (HS) state is a single determinant state, has little spin contamination, and can be easily described by standard DFT. After the energies of these two states are obtained, a weak-coupling approximation[27] maps BS-DFT energies onto the Heisenberg Hamiltonian

$$J_{AB} = \frac{E_{BS} - E_{HS}}{2S_A S_B} \quad (2)$$

This technique can be extended to the case of polymetallic systems A−B−C... by associating the various BS solutions, $\uparrow\downarrow\uparrow$..., with the appropriate Ising states and solving a set of linear equations for the *J* values.[28]


(13) Canada-Vilalta, C.; O'Brien, T. A.; Brechin, E. K.; Pink, M.; Davidson, E. R.; Christou, G. *Inorg. Chem.* **2004**, *43*, 5505−5521.
(14) Filatov, M.; Shaik, S. *Chem. Phys. Lett.* **1998**, *288*, 689−697.
(15) Grafenstein, J.; Cremer, D. *Phys. Chem. Chem. Phys.* **2000**, *2*, 2091−2103.
(16) Kortus, J.; Hellberg, C. S.; Pederson, M. R. *Phys. Rev. Lett.* **2001**, *86*, 3400−3403.
(17) Pederson, M. R.; Khanna, S. N. *Phys. Rev. B: Condens. Matter Mater. Phys.* **1999**, *60*, 9566−9572.
(18) Ruiz, E.; Rodriguez-Fortea, A.; Cano, J.; Alvarez, S. *J. Phys. Chem. Solids* **2004**, *65*, 799−803.
(19) Ruiz, E.; Cano, J.; Alvarez, S. *Polyhedron* **2005**, *24*, 2364−2367.
(20) Rajaraman, G.; Ruiz, E.; Cano, J.; Alvarez, S. *Chem. Phys. Lett.* **2005**, *415*, 6−9.
(21) Noodleman, L. *J. Chem. Phys.* **1981**, *74*, 5737−5743.
(22) Ruiz, E.; Cano, J.; Alvarez, S.; Alemany, P. *J. Am. Chem. Soc.* **1998**, *120*, 11122−11129.
(23) Soda, T.; Kitagawa, Y.; Onishi, T.; Takano, Y.; Shigeta, Y.; Nagao, H.; Yoshioka, Y.; Yamaguchi, K. *Chem. Phys. Lett.* **2000**, *319*, 223−230.
(24) Rudra, I.; Wu, Q.; Van Voorhis, T. *J. Chem. Phys.* **2006**, *24*, 024103.
(25) Kohn, W.; Sham, L. J. *Phys. Rev.* **1965**, *140*, A1133−1138.
(26) Yamaguchi, K. *Chem. Phys. Lett.* **1999**, *66*, 395−399.
(27) Sinnecker, S.; Neese, F.; Noodleman, L.; Lubitz, W. *J. Am. Chem. Soc.* **2004**, *126*, 2613−2622.
(28) Noodleman, L.; Norman, J. G.; Osbourne, J. H.; Aizman, A.; Case, D. A. *J. Am. Chem. Soc.* **1985**, *107*, 3418−3426.

Alternatively, one can assume strong coupling, which amounts to treating the BS state as if it were a spin eigenstate, which results in an unprojected BS-DFT formula[22,29,30]

$$J_{AB} = \frac{E_{BS} - E_{HS}}{2S_A S_B + S_B} \tag{3}$$

In many antiferromagnetic complexes, the exchange coupling $J$ is overestimated by the original (projected) approach. As a result, the unprojected approach often gives better agreement with experiment because it always reduces the magnitude of $J$ relative to the projected method irrespective of the nature of exchange interaction or molecular structure.

We have recently proposed an alternative to BS-DFT calculations based on the formalism of constrained DFT.[24] The primary problem with BS-DFT is that the BS solution is not an accurate representation of the $|\uparrow\downarrow\rangle$ state. BS-DFT tends to delocalize electrons due to the self-interaction error (SIE) present in approximate exchange correlation functionals. This leads to overstabilization of LS states and an overestimation of antiferromagnetic $J$ values. The pragmatic success of BS-DFT depends in many cases on a fortuitous cancellation of this SIE and the static correlation missing in the KS determinant—a cancellation that is only partially successful in practice.[31,32] In fact, there is significant debate about the extent to which this cancellation can be assumed[31,33] and what types of correlation SIE actually mimics.[32,34,35] One way to circumvent these uncertainties would be to obtain an alternative and more rigorous representation of the $|\uparrow\downarrow\rangle$ Ising spin state than the one provided by BS-DFT. To this end, assume a complex A−B can be divided into two fragments A and B with spins $S_A$ and $S_B$, respectively. We obtain the $|\uparrow\downarrow\rangle$ state directly by minimizing the KS energy subject to the constraint that the spin of A (i.e., the difference between the number of $\uparrow$ ($N_A^\alpha$) and $\downarrow$ ($N_A^\beta$) electrons on A) should be $S_A$ and the spin on B should be $-S_B$. Similarly, the HS $|\uparrow\uparrow\rangle$ state is obtained by constraining $+S_A/+S_B$. These constrained DFT solutions are *not* approximations to the spin eigenstates of the system, as the constraints placed on the system break spin symmetry and essentially preclude the convergence to a pure spin state. Instead, these states are the *Ising* configurations of the system. As a result, the constrained states are much easier to approximate with a single determinant, have less static correlation, and are less strongly influenced by SIE.[24,36] The constrained states are also well-suited to the original weak-coupling prescription for computing $J$:

$$J_{AB} = \frac{E_{\uparrow\downarrow} - E_{\uparrow\uparrow}}{2S_A S_B} \tag{4}$$

This has previously been shown to be successful in describing exchange couplings in metal dimer compounds. In this paper, we extend the C-DFT approach to polymetallic systems in strict analogy to BS-DFT. Thus, for a many-centered molecule A−B−C..., we obtain a number of Ising solutions, $\uparrow\downarrow\uparrow\uparrow$.., using constraints and obtain the $J$ values by solving a set of linear equations (see below).

We note two important theoretical points before discussing the chemistry of these compounds. The first is that, for systems with more than three centers, there are more Ising solutions $\uparrow\downarrow\uparrow\uparrow$... than there are exchange parameters $J_{ij}$. Thus, the exchange parameters are *overdetermined*, and the computed exchange couplings will generally depend on the configurations chosen to extract the $J$ values. In our opinion, this is a point that is not sufficiently stressed in the literature, and we discuss it in some depth in the applications below. Because the Heisenberg Hamiltonian (eq 1) is known to be a good approximation for molecular magnets with localized spin moments, we will interpret any deviation of the energies computed in this paper from those predicted by eq 1 as a weakness of the *ab initio* approach. This perspective is not universal—there are numerous molecules where the standard Heisenberg form is known to be inadequate and in these cases the unusual spin interactions are critically determined by ab initio data. However, for the present work we have intentionally chosen molecules where eq 1 is expected to work very well so that discrepancies between computed energies and the Heisenberg predictions will in fact reflect an inconsistency of the computed energies.

The second point we wish to make is that the formal benefits of applying constraints to the system become readily apparent when dealing with frustrated polymetallic systems. In these cases, there is a *manifold* of important low-lying ground and excited spin states with the same $\hat{S}^2$ and $M_S$ values. Since KS DFT is a ground-state method, only the *lowest energy* state with a given total spin is guaranteed to be correct. Thus, left to itself, DFT is not expected to correctly predict the energies of all the spin eigenstates associated with the Heisenberg Hamiltonian. This point does not keep a prescription such as BS-DFT from being useful and even accurate in practice, but it does present a formal obstacle: Typically, for each system one finds a number of different BS solutions with the same $M_S$ value, and only one of them (the lowest one) is known to have the correct formal energy. In particular, it is not clear that improving the functional will necessarily make the higher BS solutions better, since it is not known whether the exact functional predicts these states correctly or not. Fortunately, by applying constraints to the system, one can obtain the energies of all the Ising configurations as *ground states* of the system under different potentials, circumventing the direct calculation of any excited states. The Ising configurations, in turn, are sufficient to determine the $J$ values and hence indirectly predict the energies of the excited states. This illustration supports the general conclusion that C-DFT allows one to

(29) Ruiz, E.; Rodriguez-Fortea, A.; Cano, J.; Alvarez, S.; Alemany, P. *J. Comput. Chem.* **2003**, *24*, 982−989.
(30) Ruiz, E. *Struct. Bonding* **2004**, *113*, 71−102.
(31) Ruiz, E.; Alvarez, S.; Cano, J.; Polo, V. *J. Chem. Phys.* **2005**, *123*, 164110.
(32) Polo, V.; Kraka, E.; Cremer, D. *Theor. Chem. Acc.* **2002**, *107*, 291−303.
(33) Adamo, C.; Barone, V.; Bencini, A.; Broer, R.; Filatov, M.; Harrison, N. M.; Illas, F.; Malrieu, J. P.; Moreira, I. D. R. *J. Chem. Phys.* **2006**, *124*, 107101.
(34) Polo, V.; Kraka, E.; Cremer, D. *Mol. Phys.* **2002**, *100*, 1771−1790.
(35) Cremer, D. *Mol. Phys.* **2001**, *99*, 1899−1940.
(36) Behler, J.; Delley, B.; Lorenz, K.; Scheffler, M. *Phys. Rev. Lett.* **2005**, *94*, 036104.

obtain excited-state information from an essentially ground-state technique. Now, these formal considerations may or may not have an impact in practice; it may be that, while never exact, the BS solutions are nevertheless accurate enough with existing functionals that good exchange couplings can be obtained. Indeed, BS-DFT has been shown to give satisfactory exchange couplings in numerous polymetallic systems.[37−39] In these cases, one would expect C-DFT to add little or nothing to the calculation. However, in cases where BS-DFT is inadequate, it is important to realize that one possible source of inaccuracy is the fact that, while BS-DFT is a fairly good approximation, it may not carry over into an exact result even if the exact functional is used.

## III. Computational Methodology

In all our BS and constrained calculations we have used the B3LYP exchange-correlation functional,[40] which has previously been shown to give the best exchange couplings compared with other widely used functionals.[41] The atomic coordinates are taken directly from the crystal structure data, rather than being re-optimized, to avoid any errors that might come from differences between the theoretical and experimental structures. We have used Ahlrich's TZV basis for the metal ions and Ahlrich's VDZ basis for ligand atoms.[42,43] This is consistent with our previous work.[24] All of the C-DFT calculations were performed with *NWChem*[44] while the BS-DFT calculations were performed using *Gaussian 03*.[45] To generate the BS-DFT solutions, we first ran the HS calculation and identified the molecular orbitals (MO) that were mostly localized on metal ions. We then flipped the spins in these orbitals depending on which metal spin is ↓ in the desired BS configuration and used this as an initial guess for the BS calculation. We should note that no initial guess manipulation needed to be done to *any* of the C-DFT calculations. In all cases, the spin symmetry is broken spontaneously by the constraining potential[24] without altering the initial guess orbitals. In some cases it was advantageous to use the C-DFT orbitals as an initial guess for the BS calculations to ensure that the BS results were converged to the lowest state.

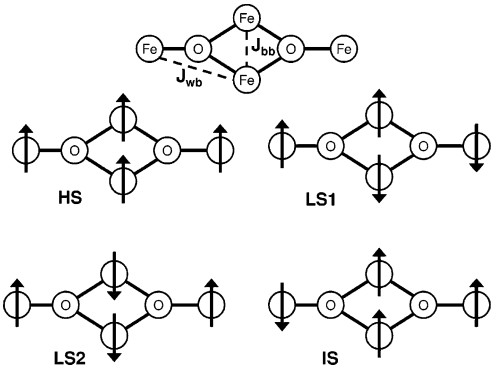


**Figure 1.** Low-lying spin states for a $Fe_4$ complex.

## IV. Extracting *J* Couplings

Assuming that the excess spin is localized on the metal atoms, DFT states are naturally associated with Ising spin configurations. For example, Figure 1 shows the low-lying states for an $Fe_4$ complex where each site has $S = {}^5/_2$ and the Heisenberg Hamiltonian is given by

$$\hat{H} = E_0 - J_{wb}(\mathbf{S}_1\cdot\mathbf{S}_2 + \mathbf{S}_2\cdot\mathbf{S}_3 + \mathbf{S}_3\cdot\mathbf{S}_4 + \mathbf{S}_4\cdot\mathbf{S}_1) - J_{bb}(\mathbf{S}_1\cdot\mathbf{S}_3) \quad (5)$$

where we have explicitly included the zero of energy which is implicitly present in the calculations. We discuss this system in detail below, but for now we use it to illustrate how exchange couplings can be extracted from the Ising configurations. There are two low-spin (LS1 and LS2) configurations with $M_S = 0$, one intermediate spin (IS) configuration with $M_S = 5$, and one HS configuration with $M_S = 10$. We can explicitly write the energies of these configurations in terms of coupling constants $J_{wb}$ and $J_{bb}$ using the Ising form of the Heisenberg Hamiltonian, as shown in Figure 1. Thus,

$$\begin{aligned} E_{LS1} &= E_0 + 25/4J_{bb} \\ E_{LS2} &= E_0 + 25J_{wb} - 25/4J_{bb} \\ E_{IS} &= E_0 - 25/4J_{bb} \\ E_{HS} &= E_0 - 25J_{wb} - 25/4J_{bb} \end{aligned} \quad (6)$$

In the original (projected) BS-DFT approach, the energies on the left-hand sides are associated with the corresponding BS solutions. In our approach, each of these energies is instead identified with the energy of the appropriate constrained DFT Ising configuration. In this way, our prescription will remove unwanted SIE from the calculation and reduce the multireference character of the target states. One expects that this will improve the quality of the predictions in the same manner as for dimers.[24] Now, we require three equations to determine the two unknown exchange couplings $J_{wb}$ and $J_{bb}$ together with the overall zero level of energy, $E_0$. Thus, the system of equations eq 6 is *overdetermined*.


(37) Mouesca, J. M.; Noodleman, L.; Case, D. A. *Int. J. Quantum Chem.* **1995**, *S22*, 95−102.
(38) Schmitt, E. A.; Noodleman, L.; Baerends, E. J.; Hendrickson, D. N. *J. Am. Chem. Soc.* **1992**, *114*, 6109−6119.
(39) Adams, D. M.; Noodleman, L.; Hendrickson, D. N. *Inorg. Chem.* **1997**, *36*, 3966−3984.
(40) Becke, A. D. *J. Chem. Phys.* **1993**, *98*, 5648−5652.
(41) Ruiz, E.; Alemany, P.; Alvarez, S.; Cano, J. *J. Am. Chem. Soc.* **1997**, *119*, 1297−1303.
(42) Schafer, A.; Huber, C.; Ahlrichs, R. *J. Chem. Phys.* **1994**, *100*, 5829−5835.
(43) Schafer, A.; Horn, H.; Ahlrichs, R. *J. Chem. Phys.* **1992**, *97*, 2571−2577.
(44) High Performance Computational Chemistry Group. *NWChem, A Computational Chemistry Package for Parallel Computers*, version 4.6; Pacific Northwest National Laboratory: Richland, WA, 2004.
(45) Frisch, M. J.; Trucks, G. W.; Schlegel, H. B.; Scuseria, G. E.; Robb, M. A.; Cheeseman, J. R.; Montgomery, J. A., Jr.; Vreven, T.; Kudin, K. N.; Burant, J. C.; Millam, J. M.; Iyengar, S. S.; Tomasi, J.; Barone, V.; Mennucci, B.; Cossi, M.; Scalmani, G.; Rega, N.; Petersson, G. A.; Nakatsuji, H.; Hada, M.; Ehara, M.; Toyota, K.; Fukuda, R.; Hasegawa, J.; Ishida, M.; Nakajima, T.; Honda, Y.; Kitao, O.; Nakai, H.; Klene, M.; Li, X.; Knox, J. E.; Hratchian, H. P.; Cross, J. B.; Bakken, V.; Adamo, C.; Jaramillo, J.; Gomperts, R.; Stratmann, R. E.; Yazyev, O.; Austin, A. J.; Cammi, R.; Pomelli, C.; Ochterski, J. W.; Ayala, P. Y.; Morokuma, K.; Voth, G. A.; Salvador, P.; Dannenberg, J. J.; Zakrzewski, V. G.; Dapprich, S.; Daniels, A. D.; Strain, M. C.; Farkas, O.; Malick, D. K.; Rabuck, A. D.; Raghavachari, K.; Foresman, J. B.; Ortiz, J. V.; Cui, Q.; Baboul, A. G.; Clifford, S.; Cioslowski, J.; Stefanov, B. B.; Liu, G.; Liashenko, A.; Piskorz, P.; Komaromi, I.; Martin, R. L.; Fox, D. J.; Keith, T.; Al-Laham, M. A.; Peng, C. Y.; Nanayakkara, A.; Challacombe, M.; Gill, P. M. W.; Johnson, B.; Chen, W.; Wong, M. W.; Gonzalez, C.; Pople, J. A. *Gaussian 03*; Gaussian, Inc.: Pittsburgh, PA.

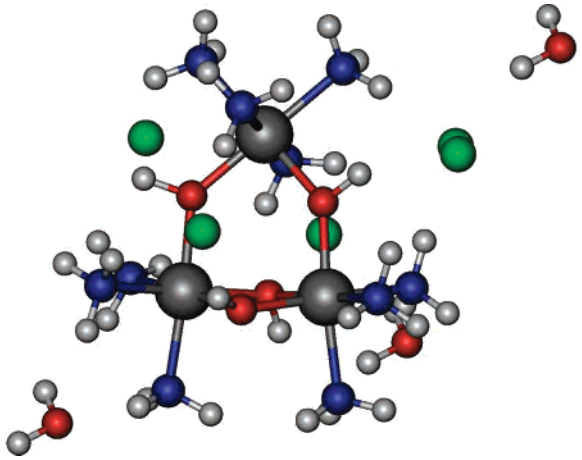

**Figure 2.** Structure of $Cr_3$ complex where Cr1 (top) is exchange coupled with Cr2 and Cr3 (bottom) via exchange interaction $J$ and Cr2 is exchange coupled with Cr3 via $J'$.

The typical solution is to choose three of the energies to determine the $J$ values. For example, if we use $E_{LS1}$, $E_{LS2}$, and $E_{HS}$ we obtain

$$J_{bb} = \frac{2E_{LS1} - E_{HS} - E_{LS2}}{25} \quad J_{wb} = \frac{E_{LS2} - E_{HS}}{50} \qquad (7)$$

However there are, of course, four different ways to choose three energies from four possibilities. If the Heisenberg Hamiltonian is truly accurate for a polymetallic cluster, all of these choices should give the same or at least nearly the same $J$ values. Thus, for the systems studied below, large variations in the $J$ values determined by selecting different configurations will be a sign of inconsistency in the underlying calculations. Obviously, the more accurate the DFT descriptions of LS1, LS2, IS, and HS are, the smaller will be the variance between the predicted $J$ values.

## V. Results and Discussion

**A. Trinuclear Chromium Cluster with Spin Frustration.** This complex, $[Cr_3(NH_3)_{10}(OH)_4]\cdot Br_5$, has $Cr^{III}$ ions arranged in an isosceles triangular arrangement, coupled to each other antiferromagnetically via $\mu$-hydroxo bridges.[46] Each $Cr^{III}$ ion is hexacoordinated. Both Cr2 and Cr3 are covalently attached to three OH and three $NH_3$ ligands while Cr1 is covalently linked to two OH and four $NH_3$ ligands (see Figure 2). This cluster is a typical example of a frustrated system due to its geometry (Figure 2) which gives rise to competing exchange pathways. As a result, the energy levels are very closely spaced and the nature of the ground state delicately depends on the relative strengths of the exchange interactions. From experiments it is known that this complex has a quartet (spin $^3/_2$) ground state. The magnetic interactions between three $Cr^{III}$ ions can be described using the following Heisenberg Hamiltonian

$$\hat{H} = -J(\mathbf{S}_1\cdot\mathbf{S}_2 + \mathbf{S}_1\cdot\mathbf{S}_3) - J'(\mathbf{S}_2\cdot\mathbf{S}_3) \qquad (8)$$

$J$ and $J'$ are experimentally determined to be equal to $-18.7$ and $-7.9$ cm$^{-1}$, respectively.[46] Solving eq 8 by diagonalizing the spin Hamiltonian and analyzing the eigenvalues and eigenstates carefully, one finds that for the ratio of $J/J' \geq {}^3/_2$ the ground state of the cluster is a quartet whereas if the ratio is smaller than $^3/_2$ a doublet becomes the ground state. This is the clear manifestation of geometry-induced spin frustration which is observed also by Wei et al.[47] Thus, besides their absolute values, the ratio of exchange coupling parameters needs to be predicted accurately.

To compute $J$ and $J'$ using DFT, first we obtain energies of three different spin configurations, the high-spin (HS) state $|^3/_2\ ^3/_2\ ^3/_2\rangle$ and low-spin states (LS1) $|-^3/_2\ ^3/_2\ ^3/_2\rangle$ and (LS2) $|^3/_2\ -^3/_2\ ^3/_2\rangle$. Next, we calculate $J$ and $J'$ by solving a set of three linear equations following a procedure similar to that described above for $Fe_4$, which in this case does not involve any overcompleteness. $J$ and $J'$ values from Noodleman's BS-DFT approach are $-32$ and $-26$ cm$^{-1}$, respectively, which incorrectly predicts a doublet ground state. On the other hand, C-DFT predicts a correct ground state (quartet) with $J$ and $J'$ values $-14$ and $-8$ cm$^{-1}$, respectively. The fact that relative strengths of exchange coupling parameters ($J$ and $J'$) are so near the critical ratio of $^3/_2$ explains the incorrect ordering predicted by BS-DFT. It is important to note that by following a different mapping approach (e.g., Ruiz's) for BS-DFT, calculations will only change the absolute values of $J$ and $J'$ but not their ratio, which means that any BS-DFT variant will obtain the wrong ground state in this case.

We have analyzed the spin density and MO energies obtained from both approaches to understand the microscopic origin of the exchange differences. We find for the HS state that the spin density is mainly centered on the Cr atoms. Both BS-DFT and C-DFT give similar spin density pictures of the HS state. Looking at the MOs of the HS state, we find that several occupied MOs close to the highest-occupied MO have contributions mainly from $Br^-$ p orbitals, which is common in many metal halide complexes. In this complex, $Br^-$ acts as an anion outside the coordination sphere. Just below the Br MOs, we can identify energetically closely spaced occupied MOs with mainly Cr d character separated from primarily ligand-centered orbitals. These metal-centered MOs carry three unpaired d electrons per Cr atom contributing primarily to the spin density.

In contrast, for LS1 and LS2, BS-DFT and C-DFT give qualitatively different results. In particular, for LS1, BS-DFT predicts an unphysical $\beta$ spin density on Br (Figure 3). This is perhaps not surprising given that the frontier orbital in the HS complex was primarily localized on Br. Indeed, in LS1 a $\beta$ MO with Br p character intrudes into the three energetically closely spaced Cr d $\beta$ MOs. By contrast, for C-DFT, Figure 3 clearly shows that the excess spin is localized on the Cr atoms. This is consistent with the fact that, in the constrained calculations, the Br p orbitals always remain energetically separated from the closely spaced $\alpha$ or $\beta$ MOs of Cr d character. We note that in practice it is virtually impossible to ensure that any given BS-DFT solution is the global minimum and not simply a local

(46) Andersen, P.; Damhus, T.; Pedersen, E.; Petersen, A. *Acta Chem. Scand.* **1984**, *38*, 359−376.
(47) Wei, H.; Wang, B.; Chen, Z. *Chem. Phys. Lett.* **2005**, *407*, 147−152.

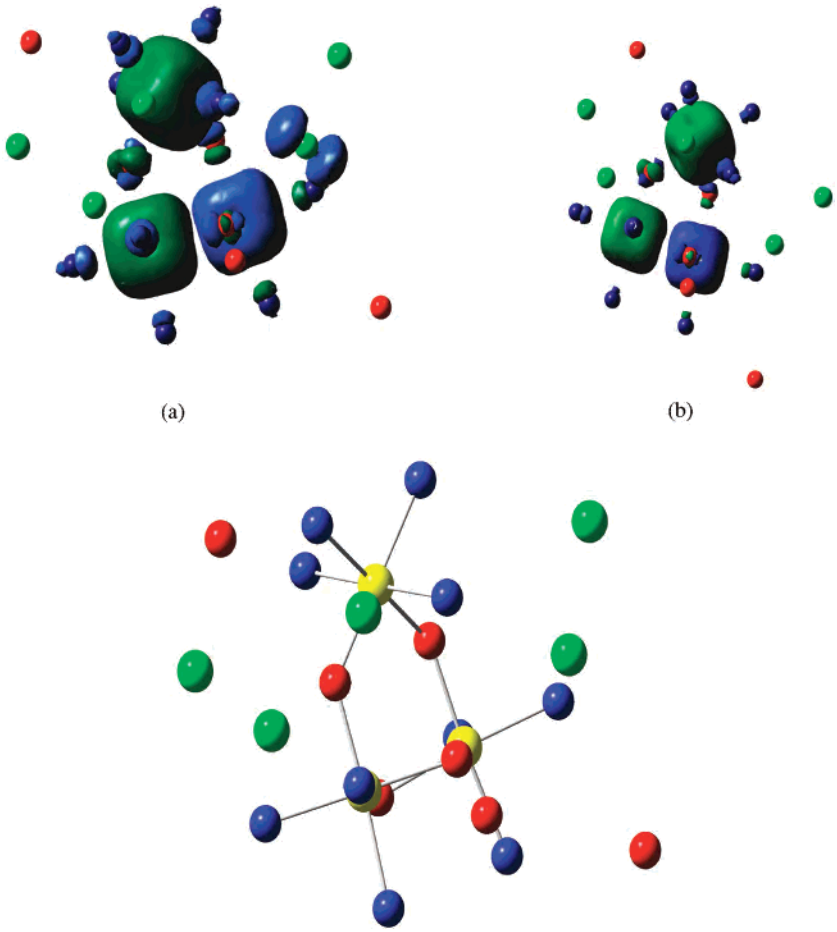


**Figure 3.** Spin density of LS1 state from BS-DFT and C-DFT calculations, respectively (a and b). Green (blue) color indicates α ($\beta$) spin density. BS-DFT predicts unphysical $\beta$ spin density on Br. Bottom figure shows a view of the coordination between the atoms from a similar perspective. Colors: yellow = Cr, red = O, blue = N, green = Br.

minimum. Thus, we cannot guarantee that there is not another BS solution for this complex that has all the spin density on the Cr atoms. We have tried choosing several different initial guesses and convergence strategies—including starting the BS calculation from the converged C-DFT orbitals—but have not succeeded in finding a more physical BS solution. Despite recent progress,[48−50] this situation remains common for BS methods; there may be multiple self-consistent solutions but it is quite difficult to control convergence, making it virtually impossible to guarantee that a given solution is the only one or even the lowest possible. As we have noted previously, this difficulty is greatly reduced in C-DFT as the constraint allows one to exert a great deal of control over the converged state.

A word should be added here about the choice of fragments in the C-DFT calculations. One must specify the groups of atoms associated with "Fragment1" (around Cr1), "Fragment2" (around Cr2), and "Fragment3" (around Cr3). The calculation then forces the net spins on these fragments to be $-^3/_2 + ^3/_2 + ^3/_2$ for LS1 (and $+^3/_2 - ^3/_2 + ^3/_2$ for LS2). One can envision two reasonable choices for these fragments: either all the atoms (including Br) are assigned to the fragment associated with the nearest Cr center or else all the atoms except the bromines are assigned in this way, leaving the bromine atoms unassigned. If we follow the latter prescription, we obtain $J = -14$ cm$^{-1}$ and $J' = -8$ cm$^{-1}$ as above whereas the former fragment choice gives $J = -26$ cm$^{-1}$ and $J' = -16$ cm$^{-1}$. Hence, both fragment prescriptions yield the same quartet ground state. Examining the spin density for the former fragment choice (not shown) indicates that some spin density is present on the Br atoms in this case, although to a lesser extent than in the BS calculations. Thus, on physical grounds, we choose as our reference the C-DFT results with fragments that do not include the Br counterions.

Thus, it seems clear that the problems with BS-DFT ground-state prediction can be tied directly to the incorrect description of the spin density in the LS1 state. The incorrect placement of the Br p orbital leads to unphysical $\beta$ spin density on Br, which artificially stabilizes LS1, resulting in a wrong $J/J'$ ratio and an incorrect ground state. By restricting attention to the physically relevant densities, C-DFT avoids these complications and predicts the correct ground state.

**B. Tetranuclear Iron Cluster with Butterfly Core.** This model complex, $[Fe_4O_2(O_2CCH_3)_7(bpy)_2]^+$, contains a but-

(48) Vacek, G.; Perry, J. K.; Langlois, J.-M. *Chem. Phys. Lett.* **1999**, *310*, 189.
(49) Lovell, T.; Li, J.; Liu, T.; Case, D. A.; Noodleman, L. *J. Am. Chem. Soc.* **2001**, *123*, 12392.
(50) Szilagyi, R. K.; Winslow, M. A. *J. Comput. Chem.* **2006**, *27*, 1385−1397.

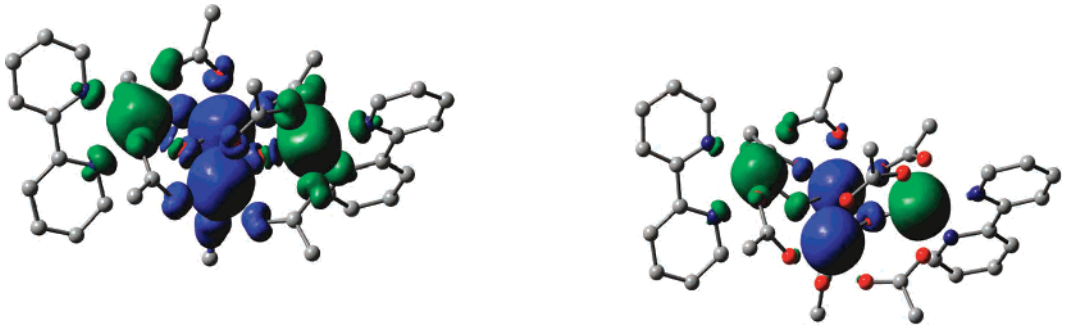

**Figure 4.** Spin density distribution of LS2 state according to BS-DFT and constrained DFT calculations, respectively. Green and blue colors have the same meaning as in Figure 3. Clearly, BS-DFT delocalizes the spin density more than C-DFT.

terfly $Fe_4^{III}O_2$ core that can be considered as two edge-sharing $Fe_3O$ triangular units with oxygen atoms slightly below the $Fe_3$ planes.[51] The separation between the central (body) Fe ions is shorter than the body−wing separation, as illustrated in Figure 1. Thus there are two types of exchange coupling in this complex, wing−body ($J_{wb}$) and body−body ($J_{bb}$) interactions. The Heisenberg Hamiltonian for this cluster is (refer to Figure 1)

$$\hat{H} = -J_{wb}(\mathbf{S}_1\cdot\mathbf{S}_2 + \mathbf{S}_2\cdot\mathbf{S}_3 + \mathbf{S}_3\cdot\mathbf{S}_4 + \mathbf{S}_4\cdot\mathbf{S}_1) - J_{bb}(\mathbf{S}_1\cdot\mathbf{S}_3) \quad (9)$$

Due to strong wing−body ($J_{wb}$) coupling, the body−body interaction ($J_{bb}$) is frustrated. Experimentally, it is known that $J_{wb}$ is antiferromagnetic (AFM) ($-90$ cm$^{-1}$) and $J_{bb}$ is more positive than $-30$ cm$^{-1}$ leading to a singlet ($S = 0$) ground state.[51] The exact nature of $J_{bb}$ is not determined, but considering the geometry of exchange pathway, it is postulated to be AFM. The AFM nature of $J_{bb}$ coupling is also expected according to Goodenough−Kanamori−Anderson's superexchange theory[52−54] between half-filled Fe1 and Fe3 $d^5$ orbitals mediated through O p orbitals unless the orbitals on two Fe atoms are completely orthogonal to each other. Considering that the angle Fe1−O−Fe3 is ≈95°, we can expect the AFM coupling to be fairly weak, which indeed is consistent with the experiment.

From the geometry of the cluster, we notice that we can construct four spin configurations. Two of them, $|^5/_2\ -^5/_2\ -^5/_2\ ^5/_2\rangle$ (LS1) and $|-^5/_2\ ^5/_2\ -^5/_2\ ^5/_2\rangle$ (LS2), are $M_s = 0$ states while one state, $|^5/_2\ ^5/_2\ ^5/_2\ -^5/_2\rangle$ (IS), has $M_s = 5$ and the last, $|^5/_2\ ^5/_2\ ^5/_2\ -^5/_2\rangle$ (HS), has $M_s = 10$ (refer to Figure 1). In this case, $J_{wb}$ and $J_{bb}$ are overdetermined. We will first discuss the exchange coupling values calculated using the HS and two-spin-flip states LS1 and LS2. BS-DFT calculations correctly predict the AFM coupling $J_{wb} = -102$ cm$^{-1}$ but predict an unexpected ferromagnetic (FM) coupling for $J_{bb} = +12$ cm$^{-1}$. These BS-DFT results are in reasonable agreement with previously reported BS-DFT results.[55] In comparison, C-DFT predicts both $J_{wb}$ ($= -96$ cm$^{-1}$) and $J_{bb}$ ($= -26$ cm$^{-1}$) to be AFM, which is in line with our physical picture of the correct signs of both couplings.

**Table 1.** Summary of Coupling Constants in $Fe_4$

| | $J_{wb}$ (cm$^{-1}$) | | $J_{bb}$ (cm$^{-1}$) | |
|---|---|---|---|---|
| | BS-DFT | C-DFT | BS-DFT | C-DFT |
| HS, LS1, LS2 | −102 | −96 | +12 | −26 |
| HS, LS1, IS | −88 | −92 | −12 | −34 |

In order to analyze the reason for these differences, we first take a look at the energies of the spin states (HS, LS1, LS2 ,IS) predicted by these two approaches. The main difference in the state ordering is that both LS1 and LS2 are preferentially stabilized in BS-DFT compared with C-DFT. From the spin densities of LS2 (Figure 4), it is clear that BS-DFT and C-DFT give qualitatively similar descriptions of the density of LS2. However, the spin for BS-DFT is quantitatively more delocalized than that for C-DFT, and this delocalization will stabilize the AFM state relative to the FM state in the standard way.[31] A similar argument applies to LS1.

In this example, we again find that BS-DFT is not able to predict the correct energy level ordering of the spin eigenstates because of errors in describing LS Ising configurations (LS1 and LS2). This is to be expected, because LS states typically involve multiconfigurational wavefunctions that are poorly described in DFT. As an obvious improvement, one can try determining coupling constants using states with higher $M_S$ values, which will have less multiconfigurational character. Therefore, we now look into the possibility of using the energy of intermediate spin-flipped-state IS to determine the coupling constants.First, we note that due to linear dependence, one cannot determine both exchange couplings from HS, LS2, and IS. However, using the BS-DFT energies of LS1, IS, and HS, we obtain $J_{wb} = -88$ cm$^{-1}$ and $J_{bb} = -12$ cm$^{-1}$ (Table 1). Thus, if we use the IS state instead of the LS2 state, $J_{bb}$ is predicted to be AFM, in agreement with the experiment. This supports our initial hypothesis that using higher $M_S$ configurations can give better results, even within BS-DFT. Interestingly, we observe that the ambiguity about the sign of the $J_{bb}$ coupling can be resolved if one can simply determine the relative ordering of LS1 and IS states. If $J_{bb}$ is AFM(FM) then LS1 is lower in energy than IS. From BS-DFT, we find LS1 to be lower than IS, explaining the AFM nature of $J_{bb}$ when IS is included

(51) McCusker, J. K.; Vincent, J. B.; Schmitt, E. A.; Mino, M. L.; Shin, K.; Coggin, D. K.; Hagen, P. M.; Huffman, J. C.; Christou, G.; Hendrickson, D. N. *J. Am. Chem. Soc.* **1991**, *113*, 3012−3021.
(52) Goodenough, J. *Magnetism and the Chemical Bond;* John Wiley and Sons: New York, 1963.
(53) Kanamori, J. *Prog. Theoret. Phys. (Kyoto)* **1957**, *17*, 177−187.
(54) Anderson, P. W. *Phys. Rev.* **1959**, *115*, 2−13.
(55) Ruiz, E.; Rodriguez-Fortea, A; Cauchy, T. *J. Chem. Phys.* **2005**, *123*, 074102.

above. By performing the same HS−LS1−IS calculation using C-DFT, we obtain couplings $J_{wb} = -92$ cm$^{-1}$ and $J_{bb} = -34$ cm$^{-1}$, which are not materially different from the results obtained with HS−LS1−LS2. Thus, we find that the exchange couplings in C-DFT are not as sensitive to the configurations chosen for computing $J$. To put it another way, the C-DFT energies of the four states more closely fit the Heisenberg Hamiltonian than do the BS-DFT predictions. The fact that C-DFT treats LS and IS states with similar accuracy can be attributed to the single configurational nature of the target solutions in C-DFT.

Finally, we note that previous BS-DFT calculations of Cauchy et al.[56] on several Fe butterfly complexes suggested a non-negligible wing−wing exchange interaction, $J_{ww} = -5.8$ cm$^{-1}$, should be included in eq 9. We have also considered this possibility in our C-DFT calculations but find only a negligible coupling ($J_{ww} = -1.2$ cm$^{-1}$). The latter result is physically reasonable given the distance between the wing atoms and the lack of any ligands shared between them. We attribute the much larger $J_{ww}$ coupling from BS-DFT to the enhanced delocalization of the excess spin. Even for spatially very distant metal centers, BS-DFT prefers to delocalize the spin density in the LS states leading, in this case, to an unusually large coupling between the centers.

**C. Single-Molecule Magnet $Fe_8$.** This cluster containing eight $Fe^{III}$ ions, of formula $[(tacn)_6Fe_8(\mu_3\text{-}O)_2(\mu_2\text{-}OH)_{12}]Br_7\text{-}(H_2O)^+$ also has a butterfly structure with Fe ions bridged by oxo and hydroxo groups.[57] Interesting phenomena of fundamental interest such as macroscopic quantum tunneling,[58] steplike hysteresis,[59] etc., along with the potential applicability for magnetic data storage devices[1] have recently created significant interest in single-molecule magnets such as $Fe_8$. In $Fe_8$, there is no rigorous symmetry, although the eight $Fe^{III}$ ions (spin $^5/_2$) are not far from $D_2$ symmetry as far as exchange pathways are concerned. Considering this, there are four unique exchange couplings which are thought to be AFM, based on the magnetic susceptibility.[57] The early susceptibility predictions have been further supported in more recent polarized neutron diffraction (PND),[60] NMR,[61] and high-frequency electron paramagnetic resonance (EPR)[62] experiments. The resulting Heisenberg Hamiltonian for $Fe_8$ can be written as

$$\hat{H} = -J_1(\mathbf{S}_2\cdot\mathbf{S}_4 + \mathbf{S}_4\cdot\mathbf{S}_6 + \mathbf{S}_6\cdot\mathbf{S}_8 + \mathbf{S}_2\cdot\mathbf{S}_8) - J_2\mathbf{S}_2\cdot\mathbf{S}_6 - J_3(\mathbf{S}_1\cdot\mathbf{S}_8 + \mathbf{S}_7\cdot\mathbf{S}_8 + \mathbf{S}_3\cdot\mathbf{S}_4 + \mathbf{S}_4\cdot\mathbf{S}_5) - J_4(\mathbf{S}_1\cdot\mathbf{S}_2 + \mathbf{S}_2\cdot\mathbf{S}_3 + \mathbf{S}_5\cdot\mathbf{S}_6 + \mathbf{S}_6\cdot\mathbf{S}_7) \quad (10)$$

Depending upon the experiment, the various exchange couplings have been estimated to be in the ranges $-120 \geq J_1$ (cm$^{-1}$) $\geq -140$, $-20 \geq J_2$ (cm$^{-1}$) $\geq -25$, $-35 \geq J_3$ (cm$^{-1}$) $\geq -41$, and $-15 \geq J_4$ (cm$^{-1}$) $\geq -18$ [57, 60−62]. In each case, the couplings were obtained by fitting the magnetic susceptibility curve, in some instances augmented by anisotropy corrections[62] or the constraint that the spin excitation gap be predicted correctly.[60] The relatively narrow range of values postulated in the various experiments supports their accuracy, as does the similarity of the various exchange couplings to analogous couplings found in other $\mu$-oxo and $\mu$-hydroxo $Fe^{III}$ pairs.[62] However, it is evident that the geometry and AFM exchange result in spin frustration which then leads to a ferrimagnetic intermediate spin (spin 10) ground state. Due to strong spin frustration changing the weaker $J$ values by a few cm$^{-1}$ or sometimes even changing the nature of these interactions (e.g., AFM to FM), this tends to have very little effect on the low-energy spectrum of the complex and the resulting magnetic susceptibility. Thus, the experimental values for the $Fe_8$ exchange couplings should be considered proposed values that are open to further validation and testing.

Previous BS-DFT calculations[63] predict a FM $J_2$ value of $+5$ cm$^{-1}$ and a considerably smaller $J_1$ value of $-67$ cm$^{-1}$ as compared to experiment[57,61] and previous theoretical calculations.[64] Meanwhile, $J_3$ and $J_4$ were determined to be $-34$ and $-11$ cm$^{-1}$, respectively, using BS-DFT. It is important to remember that due to the strong frustration experimentally present in $Fe_8$, it is difficult to unambiguously distinguish between the weak AFM and the weak FM nature of $J_2$ coupling, and therefore, the discrepancy here should properly be considered a *disagreement* of theory and experiment rather than simply an error in the theory and our goal is to resolve the disagreement. In particular, it is important to note that even though the BS-DFT couplings are quite different from the experimental ones, BS-DFT still gives a fairly good fit to the magnetic susceptibility curve.[63] Using these BS-DFT values in eq 10, the gap between ground state (spin 10) and first excited state (spin 9) is found to be 31 cm$^{-1}$, which is higher than the value ($17 \pm 1.5$ cm$^{-1}$) obtained from a high-resolution EPR experiment.[65] In this molecule, there are 50 unique LS states in addition to the HS state even accounting for $D_2$ symmetry. These states lead to a grossly overdetermined set of equations for the four exchange couplings, and in practice it is prohibitively time-consuming to determine all 50 states. Hence, for the present work, we focus on a selection of eight four- and two-spin-flip states (LS1−LS8, see Figure 5) in addition to the HS state. The exchange couplings are still overdetermined within this set, and we expect the conclusions drawn from this selection to agree qualitatively with what would be found by examining the complete manifold of Ising states. We have tried all the unique combinations of spin states and used them to determine the $J$ couplings. Rather than giving an exhaus-


(56) Cauchy, T.; Ruiz, E.; Alvarez, S. *J. Am. Chem. Soc.* **2006**, *128*, 15722.
(57) Delfs, C.; Gatteschi, D.; Pardi, L.; Sessoli, R.; Weighardt, K.; Hanke, D. *Inorg. Chem.* **1993**, *32*, 3099−3103.
(58) Wernsdorfer, W.; Sessoli, R. *Science* **1999**, *284*, 133−135.
(59) Sangregorio, C.; Ohm, T.; Paulsen, C.; Sessoli, R.; Gatteschi, D. *Phys. Rev. Lett.* **1997**, *78*, 4645−4648.
(60) Pontillon, Y.; Caneschi, A.; Gatteschi, D.; Sessoli, R.; Ressouche, E.; Schweizer, J.; Lelievre-Berna, E. *J. Am. Chem. Soc.* **1999**, *121*, 5342−5343.
(61) Furukawa, Y.; Kawakami, S.; Kumagai, K.; Baek, S.-H.; Borsa, F. *Phys. Rev. B: Condens. Matter Mater. Phys.* **2003**, *68*, 180405(R).
(62) Barra, A. L.; Gatteschi, D.; Sessoli, R. *Chem.—Eur. J.* **2000**, *6*, 1608−1614.
(63) Ruiz, E.; Cano, J.; Alvarez, S. *Chem.—Eur. J.* **2005**, *11*, 4767−4771.
(64) Raghu, C.; Rudra, I.; Sen, D.; Ramasesha, S. *Phys. Rev. B: Condens. Matter Mater. Phys.* **2001**, *64*, 064419.
(65) Zipse, D.; North, J. M.; Dalal, N. S.; Hill, S.; Edwards, R. S. *Phys. Rev. B: Condens. Matter Mater. Phys.* **2003**, *68*, 184408.

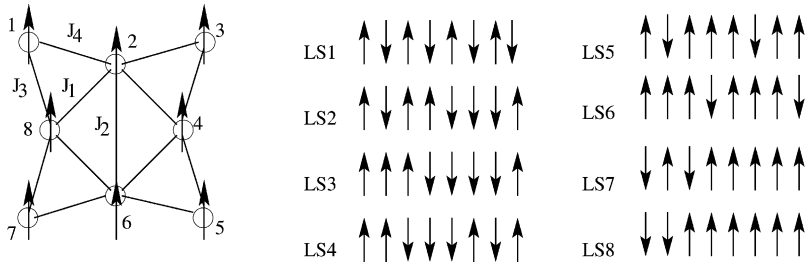


**Figure 5.** Diagram of exchange coupling interactions between spin $^5/_2$ $Fe^{III}$ ions in $Fe_8$. LS1−LS8 are different spin configurations used in the calculation.

tive list of these possibilities, below we present the range of possible predicted couplings. That is, for each $J_i$ value, we present the maximum value one can obtain, which will be realizable for one particular choice of five spin states, and the minimum value, which will be realized for another choice of states. From BS-DFT we get $-75 \geq J_1 \geq -102$ cm$^{-1}$, $+12 \geq J_2 \geq +5$ cm$^{-1}$, $-40 \geq J_3 \geq -48$ cm$^{-1}$, and $-10 \geq J_4 \geq -25$ cm$^{-1}$. Furthermore, the optical gap is between 28 and 45 cm$^{-1}$. In particular, we note that $J_1$ becomes more strongly AFM (i.e., in better agreement with experiment) when the selection of states involves two-spin-flipped configurations. Thus, BS-DFT involving higher $M_S$ states again improves the agreement with experimentally proposed values.

In contrast, using all the combinations of possible states for C-DFT, one obtains predicted exchange couplings of $-130 \geq J_1 \geq -143$ cm$^{-1}$, $-14 \geq J_2 \geq -21$ cm$^{-1}$, $-42 \geq J_3 \geq -47$ cm$^{-1}$, and $-10 \geq J_4 \geq -18$ cm$^{-1}$, in extraordinary agreement with the proposed experimental values. Here we again find that the BS-DFT results change more drastically than C-DFT values with the choice of target spin configurations, as exemplified by the large absolute change in $J_1$ and large relative shift in $J_2$ in the BS results. For C-DFT, the excitation gap between the ground state (spin 10) and first excited state (spin = 9) is calculated to be between 33 and 51 cm$^{-1}$. It is not entirely clear why the exchange couplings are in such good agreement with the experiment while the optical gap is so far off. It may in part be due to the lack of magnetic anisotropy in our model. Clearly, this is also an illustration of the extreme sensitivity of the spin states in frustrated systems to the values of the underlying exchange parameters.

We have analyzed the spin density of the lowest-energy Ising configuration (LS6 state) obtained from C-DFT (Figure 6) and compared it with the experimental PND results for the ground state.[60] We find from Löwdin population analysis that the spin density is mainly localized on the Fe atoms with some delocalization over the bridging oxo ligands, which is also found in previous BS-DFT calculations. Magnetic moments of Fe atoms at "wing-tips" (Figure 5; Fe1, Fe3, Fe5, Fe7) are larger (4.99 e$^-$) than the moments of Fe atoms at the center (Figure 5; Fe2, Fe6) sites (4.93 e$^-$). We also find negative magnetic moment (4.87 e$^-$) on the lateral Fe atoms (Figure 5; Fe4, Fe8). The trends observed in our calculated magnetic moments of different Fe ions are in good agreement with the NMR experiments.[61] The spin density structure of the ground state is an effect of spin frustration. From the PND experimental data and C-DFT

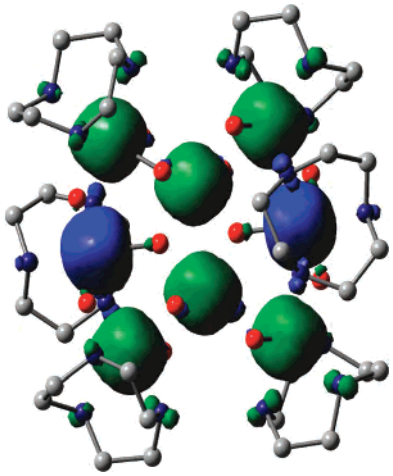

**Figure 6.** Spin density distribution of $Fe_8$ ground state from C-DFT calculations. Green and blue colors have same meaning as in Figure 3.

results, we see that all the exchange pathways are AFM in nature while their strengths are in the order $J_1 > J_3 > J_2 > J_4$. Thus, the minimum energy spin density distribution is obtained with negative spin density on Fe4 and Fe8, which satisfies all the strong AFM interactions with $J_1$ and $J_3$ couplings.

## VI. Conclusions

We have investigated the exchange couplings in three different polynuclear transition-metal complexes, $Cr_3$, $Fe_4$, and $Fe_8$. We find that an approach based on C-DFT calculations results in couplings that are in very good agreement with the experiments overall and predicts the same ordering of states as predicted in experiment. In particular, we support the quartet ground state of $Cr_3$ and the antiferromagnetic nature of $J_{bb}$ in $Fe_4$ and $J_2$ in $Fe_8$. On the other hand, BS-DFT calculations disagree with experiment on each of these key points and hence the results here appear to consistently support the experimental findings for these systems. By a detailed analysis of the spin densities in each case, we observe that the incorrect couplings appear to arise from incorrect placement of some spin density—the excess spin is more delocalized in BS-DFT and can even end up on spectator groups like Br. We hypothesize that these results stem, in part, from the difficulty of treating multiconfigurational states in BS-DFT. This is supported by the fact that using intermediate spin states (e.g., those with only one spin flipped rather than two or more) tends to give improved exchange parameters in BS-DFT. C-DFT, on the other hand, gives exchange couplings that are insensitive to the states

chosen, strongly indicating that the Heisenberg Hamiltonian is appropriate for these molecules. Theoretical confirmation of the experimental findings is particularly important in this situation, as the experimentally determined couplings typically have large uncertainties, especially for large magnetic systems. Thus, accurate theoretical tools, such as those used here, become an important means of validating the experimental results. The lone outstanding disagreement between the theoretical work here and existing experimental data arises for $Fe_8$—while the exchange constants can be predicted within the experimental error, the computed optical gap is overestimated by at least 75%. It is not clear where this error comes from, although it is worth noting that the exchange couplings are derived from magnetic susceptibility[57,60−62] while the optical gap comes from a separate set of EPR experiments.[65]

There are several important research directions suggested by the present results. The obvious task is to attempt to use the principles described here to treat more technologically relevant molecular magnets, such as $Mn_{12}$. Typically, these systems also involve significant frustration, so the principles learned here will facilitate progress. Theoretical investigations can help clarify experimental exchange constants, which are typically plagued by overparameterization problems as the number of centers grows. A second avenue would be to examine how the exchange couplings change upon charging one of the metal centers, as occurs for molecular magnets in junctions. We can study these processes by constraining not only the spin but also the charge density on each metal center. For example, interesting effects such as FM-to-AFM transitions, Kondo physics, and spin valve behavior could be tackled by determining the correct exchange constants in various charging configurations.

**Acknowledgment.** T.V.V. gratefully acknowledges funding from the National Science Foundation (CHE-0547877), the American Chemical Society (Petroleum Research Fund No. 44106-G6) the NEC Corporation, and the David and Lucille Packard Foundation.

IC700871F